

Electronic Supplementary Information (ESI)

A bifunctional fluorescent sensor for CCCP-induced cancer cell apoptosis imaging

Huawei Niu^{a,b}, Yongru Zhang^a, Jun Tang^a, Xiaofei Zhu^a, Yong Ye^{a,*}, Yufen Zhao^{a,c}

^a *Green Catalysis Center, College of Chemistry, Zhengzhou University, Zhengzhou 450001, P.R. China. E-mail: yeyong03@tsinghua.org.cn*

^b *College of Food and Bioengineering, Henan University of Science and Technology, Luoyang, 471000, China.*

^c *Institute of Drug Discovery Technology, Ningbo University, Ningbo, 450052, China.*

**Corresponding author. * yeyong03@tsinghua.org.cn (Y. Ye). Tel: 139 3907 9373*

Table of contents

Experimental

Scheme S1. The proposed mechanism of NPCF

Fig. S1 HR-MS spectrum of probe NPCF with HSO_3^-

Fig. S2 Structure characterization of NPCF

Fig. S3 Structure characterization of compound NPM

Fig. S4 UV-vis absorption spectra changes of NPCF after addition of HSO_3^-

Fig. S5 Fluorescence spectra changes of NPCF after addition of HSO_3^-

Fig. S6 Calibration curve of NPCF to HSO_3^- (0–10 equiv.)

Fig. S7 The linear responses at low HSO_3^- concentrations (0.6–1.8 equiv.)

Fig. S8 UV-vis absorption changes of NPCF in the presence of different analytes

Fig. S9 Emission changes of NPCF in the presence of different analytes

Fig. S10 The interference of NPCF towards HSO_3^- ($\lambda_{\text{ex}} = 350 \text{ nm}$)

Fig. S11 The interference of NPCF towards HSO_3^- ($\lambda_{\text{ex}} = 553 \text{ nm}$)

Fig. S12 Time-dependent fluorescence spectral changes of NPCF with HSO_3^-

Fig. S13 The effect of the pH of the test solution on the pH of NPCF

Fig. S14 UV-vis absorption spectra changes at pH 4.26 and 9.21 (NPCF and NPM)

Fig. S15 Fluorescence spectra changes at pH 4.26 and 9.21 (NPCF and NPM)

Fig. S16 Absorption spectra changes of NPCF at different pH values

Fig. S17 The pH titration curve of NPCF plotted by fluorescence as a function of pH

Fig. S18 Absorption and fluorescence spectra changes of NPM at different pH values

Fig. S19 The pH titration curve of NPM plotted by fluorescence as a function of pH

Fig. S20 The fluorescence of NPCF in pH 4.26 and 9.21 under different potential interference of interference agents

Fig. S21 Kinetic study of probe NPCF at pH 4.26 and 9.21

Fig. S22 Reversible fluorescence intensity changes of NPCF in pH 4.26-9.21

Fig. S23 Different NPCF concentrations tested in HeLa cells for toxicity

Fig. S24 Fluorescence images of MCF-7 cells for detecting exogenous HSO_3^-

Fig. S25 Fluorescence images of MCF-7 cells for detecting endogenous HSO_3^-

Fig.S26 Confocal fluorescence images of zebrafish

Fig. S27 EC1 cells imaging after incubated with SO_2 donors and LPS/PMA

Fig. S28 Confocal fluorescence images of cancer cells vs normal cells

Fig. S29 Experiments of SO_2 and pH changes in CCCP-induced apoptosis

Experimental

Materials and Methods

All chemicals were gained from reagent companies (Sigma-Aldrich, Aladdin, Macklin). Annexin V/7-AAD Apoptosis Detection Kit was gained from Shanghai Xinyu Biological Technology CO., LTD. Deionized water was used all over the work. The pH values were detected by a Model PHS-3C meter (Shanghai, China). Absorption spectrums were detected by UV-2102 double-beam UV/VIS spectrometer. Fluorescence spectrums were recorded by F-4500 FL Spectrophotometer. The ^1H NMR and ^{13}C NMR spectra were measured by Bruker DTX-400 spectrometer. ESI mass spectra were gained by an HPLC Q-Exactive HR-MS spectrometer (Thermo, USA). Flow cytometry analysis was taken on BD Canto plus (USA). Cofocal fluorescence images were gained by Zeiss LSM 880 confocal microscope.

Synthesis and characterization

Compounds **1** and **2** were gained by the literature methods.^{S1,S2}

Synthesis of probe NPCF. 240 mg of compound **1** (1.5 equiv.) and 269 mg of compound **2** (1 equiv.) were added to a flask (50 mL), followed by adding ethanol (20 mL) and piperidine (0.2 mL). After refluxing for 16 h under nitrogen, a yellow product was filtered, washed with ice-cold ethanol. 117.0 mg of **NPCF** was obtained in a yield of 28.4%. ^1H NMR (400 MHz, $\text{DMSO-}d_6$, ppm): 2.39 (s, 3H), 7.35 (t, 1H, $J = 15.0$ Hz), 7.42 (t, 1H, $J = 15.0$ Hz), 7.52 (t, 1H, $J = 15.0$ Hz), 7.60 (t, 2H, $J = 14.0$ Hz), 7.77 (s, 1H), 7.84 (s, 1H), 7.89 (d, 1H, $J = 8.1$ Hz), 8.15 (d, 1H, $J = 8.1$ Hz), 8.19–8.34 (m, 3H), 13.20 (s, 1H), 13.48 (s, 1H); ^{13}C NMR (100 MHz, $\text{DMSO-}d_6$, ppm): $\delta = 20.27, 113.33, 117.44, 121.60, 122.45, 122.77, 123.25, 123.58, 126.14, 126.46, 127.54, 129.57, 131.80, 132.83, 133.70, 135.28, 138.96, 143.57, 149.60, 151.28, 155.32, 168.84, 181.62$. HR-MS: Calcd for $[\text{C}_{24}\text{H}_{17}\text{N}_3\text{O}_2\text{S} + \text{H}]^+$: 412.1114, found 412.1117.

Synthesis of compound NPM. 269 mg of compound **2** (1 equiv.) and 553 mg of K_2CO_3 (4 equiv.) were added to a flask (50 mL), and then acetone (7 mL) were added. After refluxing for 12 h, a red-purple product was filtered, washed with acetone and deionized water. Compound **NPM** was received as a red-purple solid (136.6 mg, yield 44.2%). ^1H NMR (400 MHz, $\text{DMSO-}d_6$, ppm): 2.20 (s, 3H), 2.25 (s, 3H), 7.05 (d, 2H, $J = 16.0$ Hz), 7.21 (s, 2H), 7.36 (s, 1H), 7.79–7.93 (m, 3H), 8.02 (s, 1H); ^{13}C NMR (100 MHz, $\text{DMSO-}d_6$, ppm): $\delta = 20.73, 27.31, 115.96, 116.34, 120.74, 121.68, 121.74, 122.61, 123.69, 125.31, 131.11, 133.64, 136.11, 144.35, 152.25, 166.29, 170.87, 198.56$. HR-MS: Calcd for $[\text{C}_{18}\text{H}_{15}\text{NO}_2\text{S} + \text{H}]^+$: 310.0896, found 310.0900.

Synthesis of SO₂ donor. SO₂ donor were synthesized by reported methods.^{S3} 2, 4-dinitrobenzenesulfonyl chloride (0.594 g, 2.25 mmol) in 18 mL dry DCM at 0 °C was added to a solution of benzylamine (0.477 g, 6.0 mmol) with trimethylamine (0.963 g, 9 mmol) and 10 mL DCM, the mixture was stirred and reacted for 3 h at room temperature, then 100 mL of water was added to the solution to stop the reaction. Extracted by DCM, and the organic layer was dried by anhydrous Na₂SO₄. The solvent was removed under vacuum to get the crude product and the yellow product was collected by chromatography using DCM as eluent. SO₂ donor was obtained as a yellow solid (580.0 mg, yield 77.3%). ¹H NMR (400 MHz, CDCl₃, ppm): 4.66 (d, 2H, *J* = 5.6 Hz), 6.92 (d, 1H, *J* = 9.5 Hz), 7.34–7.42 (m, 5H), 8.20–8.24 (dd, 1H, *J* = 2.5 Hz), 8.92 (s, 1H) 9.14 (d, 1H, *J* = 2.6 Hz); ¹³C NMR (100 MHz, CDCl₃, ppm): δ = 47.58, 114.45, 124.22, 127.09, 128.37, 129.29, 130.39, 130.76, 135.59, 136.45, 148.23.

Detection Limit Calculation

For NPCF, the fluorescence intensity of 542 nm versus HSO₃⁻ concentration (0.6 to 1.8 equiv.) was investigated, and the detection limit of NPCF was counted as 22.7 nM (R² = 0.985), using the formula (1):

$$\text{Detection limit} = 3 \sigma/|k| \quad (1)$$

Cell imaging

All cells were cultured in Dulbecco's modified Eagle's medium (DMEM) supplemented with 10% fetal bovine serum at 37°C

Cytotoxicity assay. Cytotoxicity assay was executed by using Cell Counting Kit-8 (CCK-8) according to our report article.^{S4} The concentrations of NPCF changed from 0 μM to 30 μM.

Bio-imaging of NPCF for sensing HSO₃⁻ in MCF-7 cells. In order to detect endogenous HSO₃⁻, MCF-7 cells were treated with NEM (1 mM) for 0.5 h, and treated with NPCF (10 μM) for 0.5 h and SO₂ donor (100 μM) for 1h. For detecting exogenous HSO₃⁻, MCF-7 cells were incubated with NPCF (10 μM) for 0.5 h, and treated with 1equiv., 5equiv. and 10 equiv. of HSO₃⁻ for 1h, and then imaged. Conditions: λ_{ex} = 405 nm, λ_{em} = 520 nm–560 nm.

Bioimaging application of NPCF for detecting pH in HeLa cells. NPCF (10 μM) was incubated in different pH PBS buffers (pH 4.5, 5.5, 6.5, 7.5 and 8.5) for 0.5 h, and imaged by Zeiss LSM 880 confocal microscope. Conditions: λ_{ex} = 552 nm, λ_{em} = 630–670 nm.

SO₂ reduces LPS-induced inflammation and alleviates acidification environment. For the blank group, EC1 cells were incubated with NPCF (10 μM) for 0.5 h; For the control groups, EC1 cells were treated with LPS (10 mg/L) for 12 h, followed by treated with PMA (1 μg/mL) for 1 h, and imaged after incubation with NPCF (10 μM) for 0.5 h; EC1 cells were treated with SO₂ donor (100 μM) for 1 h, and then imaged after incubation with NPCF (10 μM) for 0.5 h; For the experimental group, EC1 cells were incubated with LPS (10

mg/L) for 12 h, followed by treated with PMA (1 $\mu\text{g}/\text{mL}$) for 1 h, and incubated with SO_2 donor (100 μM) for 1 h, and finally imaged after incubation with NPCF (10 μM) for 0.5 h.

Distinguishing between normal cells and cancer cells. NPCF were incubated with cancer cells (MCF-7 cells) and normal cells (MCF-10A cells) for 0.5 h, respectively, and then imaged. Conditions: for green channel, $\lambda_{\text{ex}} = 405 \text{ nm}$, $\lambda_{\text{em}} = 520 \text{ nm} - 560 \text{ nm}$; for red channel, $\lambda_{\text{ex}} = 552 \text{ nm}$, $\lambda_{\text{em}} = 630 - 670 \text{ nm}$.

Changes of SO_2 and pH in cells with the increase of CCCP concentrations. Hela cells were incubated with CCCP (Ranged from 0 μM to 30 μM) for 1 h, 12 h or 24 h, respectively. Conditions: for green channel, $\lambda_{\text{ex}} = 405 \text{ nm}$, $\lambda_{\text{em}} = 520 \text{ nm} - 560 \text{ nm}$; for red channel, $\lambda_{\text{ex}} = 552 \text{ nm}$, $\lambda_{\text{em}} = 630 - 670 \text{ nm}$.

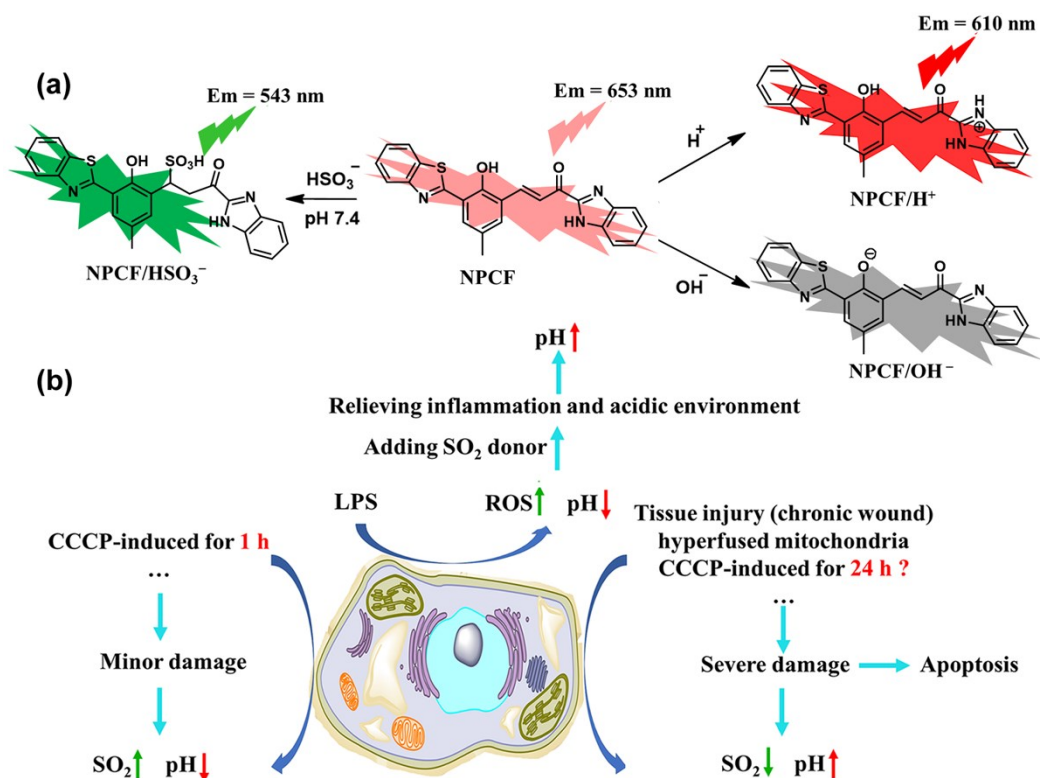
Flow cytometry analysis. Hela cells were cultured in 6-well plates at a density of 2.0×10^5 cells/well, and the cells were washed with PBS buffers and centrifuged. The cells were resuspended in PBS, stained with NPCF (10 μM) for 30 min, and checked by flow cytometry.

Zebrafish Confocal Fluorescence Imaging

Wild zebrafish were gained from Shanghai FishBio Co., Ltd. Zebrafish were fed in E3 media at 28°C . For the control groups, the two days old zebrafish were incubated with NPCF for 0.5 h and imaged. For the experimental group, zebrafish were incubated with 10 μM of NPCF for 0.5 h, treated with 100 μM of HSO_3^- for 1 h, and then imaged. Zebrafish were imaged on Zeiss LSM 880 confocal microscope. Conditions: $\lambda_{\text{ex}} = 405 \text{ nm}$, $\lambda_{\text{em}} = 520 \text{ nm} - 560 \text{ nm}$.

References

- S1 Y. Q. Ge, J. Jia, H. Yang, X. T. Tao and J. W. Wang, *Dyes Pigments*, 2011, **88**, 344-349
- S2 X. Yang, Y. Liu, Y. Wu, X. Ren, D. Zhang and Y. Ye, *Sensor. Actuat. B-Chem*, 2017, **253**, 488-494
- S3 S. R. Malwal, D. Sriram, P. Yogeeswari, V. B. Konkimalla and H. Chakrapani, *J. Med. Chem.*, 2012, **55**, 553-557.
- S4 X. Yang, W. Liu, J. Tang, P. Li, H. Weng, Y. Ye, M. Xian, B. Tang and Y. Zhao, *Chem. Commun.*, 2018, **54**, 11387-11390.



Scheme S1. The proposed mechanism of NPCF (10 μM) for detecting both HSO_3^- and pH. (b) Changes in pH during SO_2 relieving inflammation and dual indicators to detect changes in SO_2 and pH during the apoptotic process in living cells.

Fig. S1 HR-MS spectrum of probe NPCF with HSO_3^-

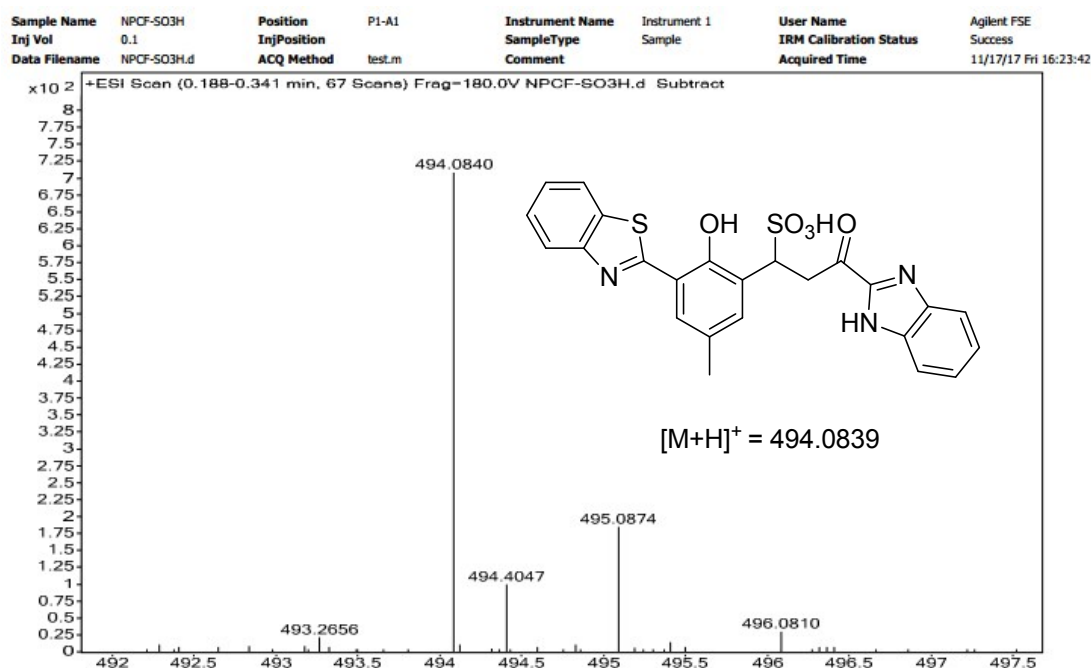
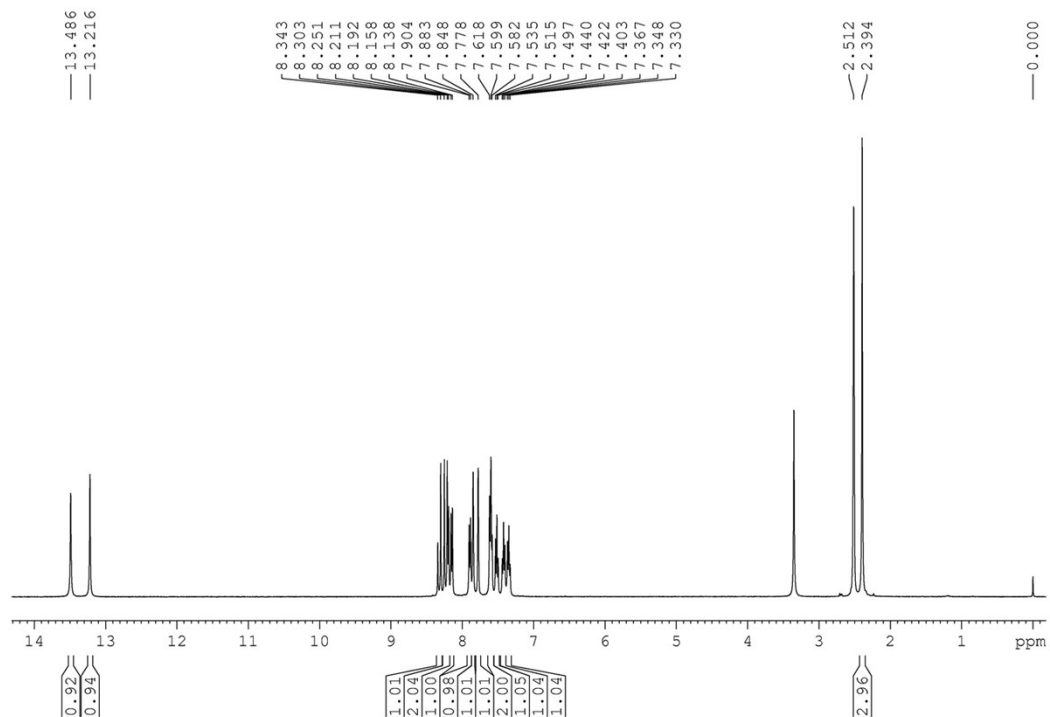
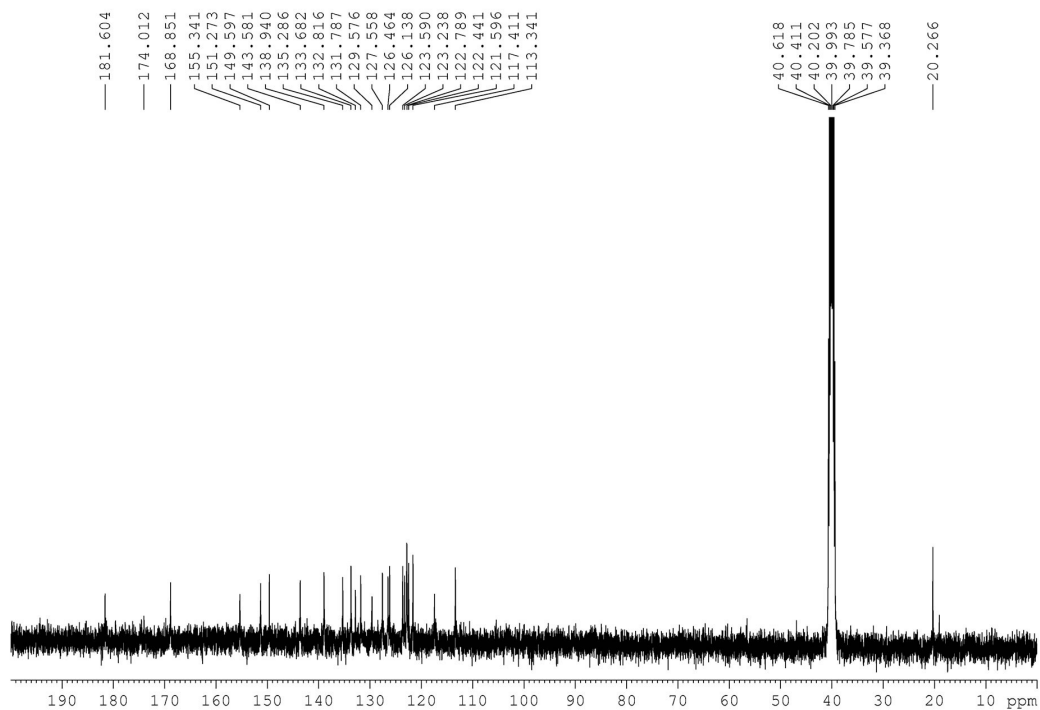


Fig. S2 Structure characterization of probe NPCF

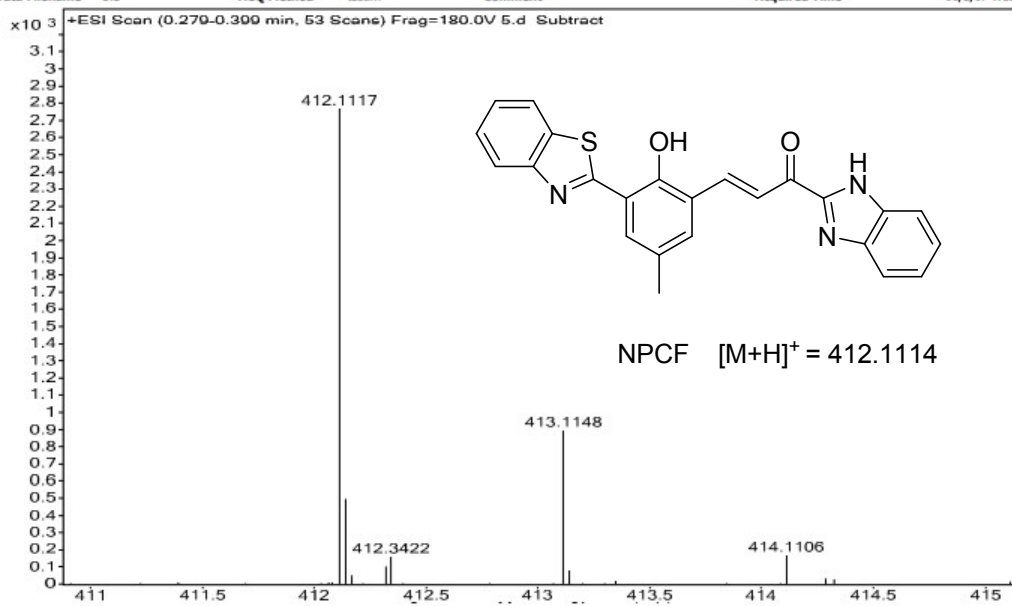


$^1\text{H-NMR}$ spectrum of probe NPCF in $\text{DMSO-}d_6$



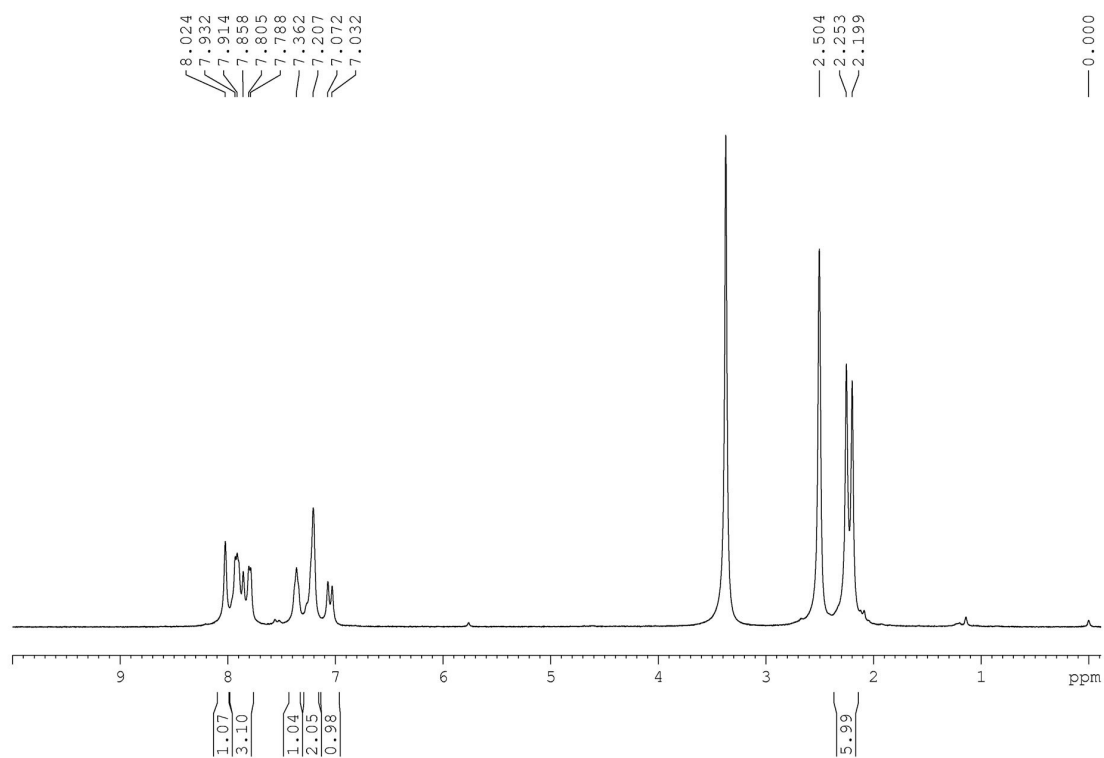
$^{13}\text{C-NMR}$ spectrum of probe NPCF in $\text{DMSO-}d_6$

Sample Name	5	Position	P1-A4	Instrument Name	Instrument 1	User Name	Agilent FSE
Inj Vol	0.1	InjPosition		SampleType	Sample	IRM Calibration Status	Success
Data Filename	5.d	ACQ Method	test.m	Comment		Acquired Time	11/8/17 Wed 16:09:35

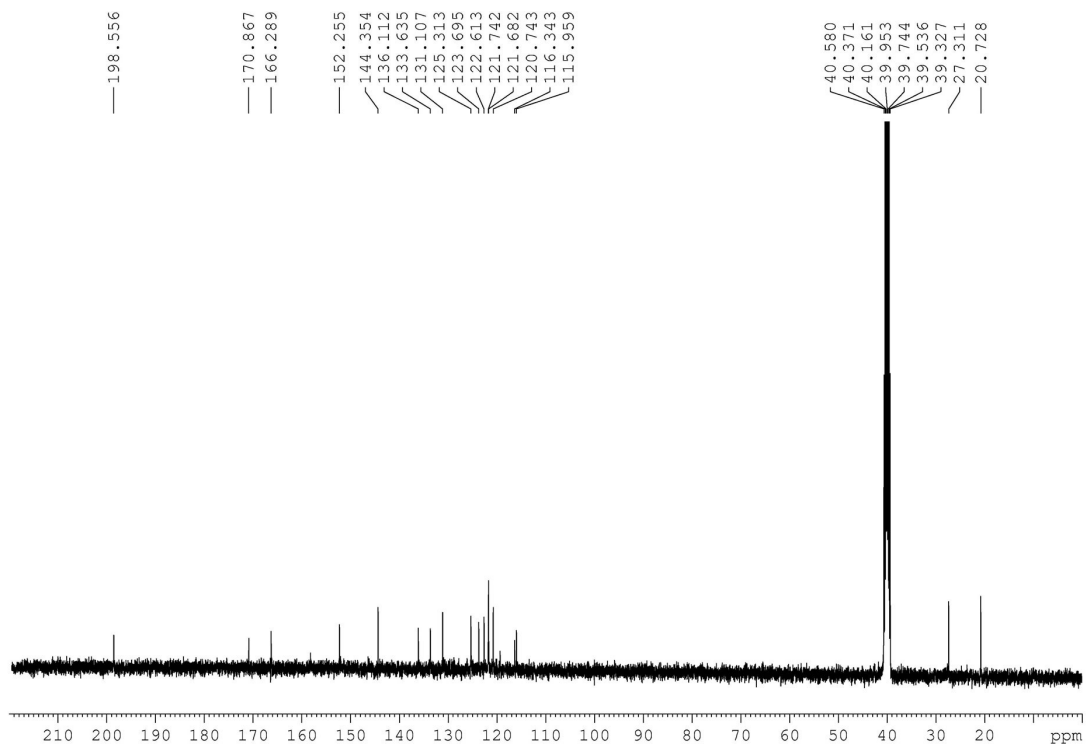


HR-MS spectrum of probe NPCF

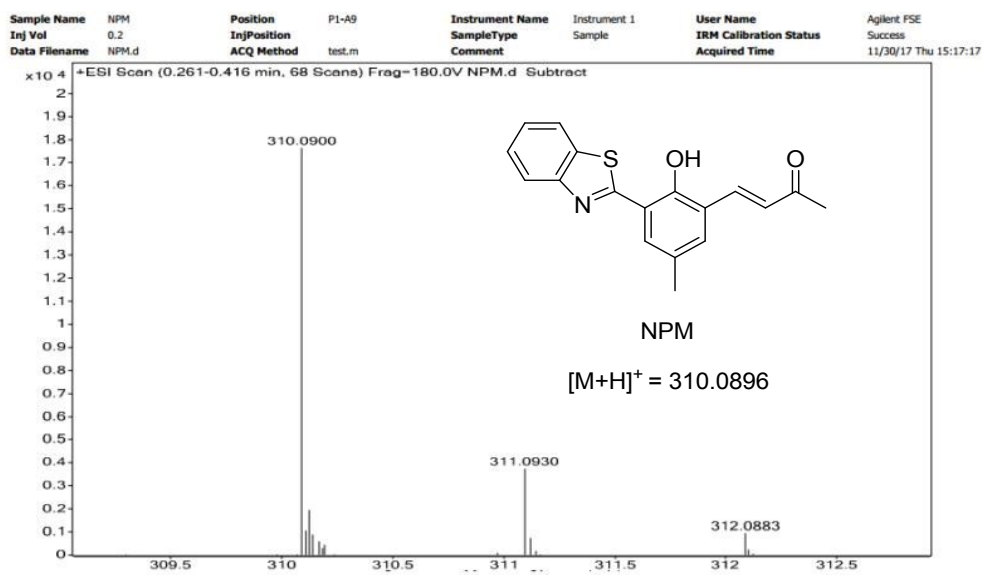
Fig. S3 Structure characterization of compound NPM



¹H-NMR spectrum of compound NPM in DMSO-*d*₆



^{13}C -NMR spectrum of compound NPM in $\text{DMSO}-d_6$



HR-MS spectrum of probe NPM

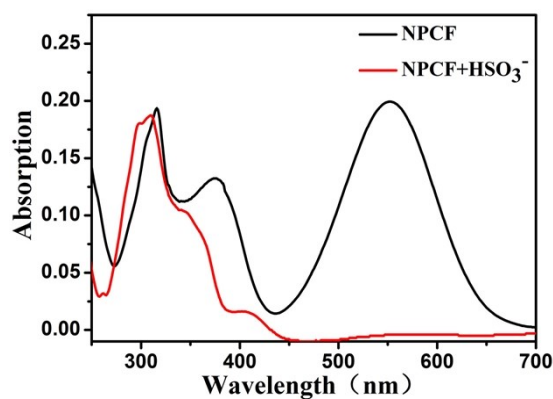


Fig. S4 UV-vis absorption spectra changes. The black line means only NPCF was added, the red line means NPCF and 10 equiv. of HSO₃⁻ were added.

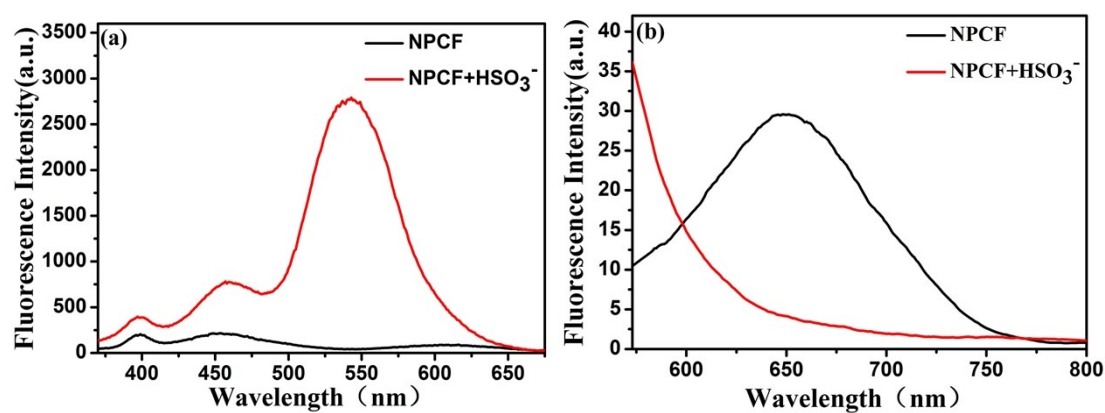


Fig. S5 (a) $\lambda_{\text{ex}} = 350 \text{ nm}$, $\lambda_{\text{em}} = 542 \text{ nm}$, slit: 10 nm/10 nm. (b) $\lambda_{\text{ex}} = 543 \text{ nm}$, $\lambda_{\text{em}} = 653 \text{ nm}$, slit: 10 nm/10 nm. All data were acquired in HEPES buffer solution (pH = 7.4, 10 mM, containing 1 mM CTAB). The black line means only NPCF was added, the red line means NPCF and 10 equiv of HSO₃⁻ were added.

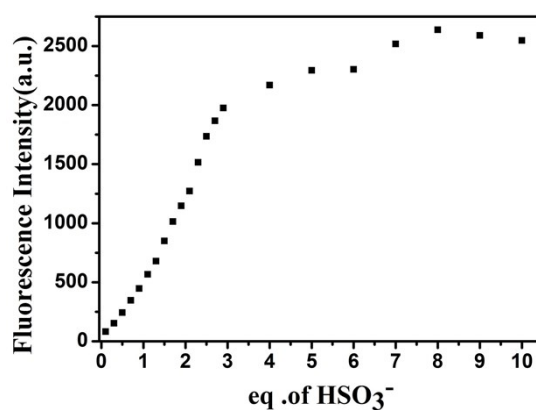


Fig. S6 Calibration curve of probe NPCF to HSO₃⁻ (0–10 equiv.). Conditions: $\lambda_{\text{ex}} = 350 \text{ nm}$, slit: 10 nm/10 nm.

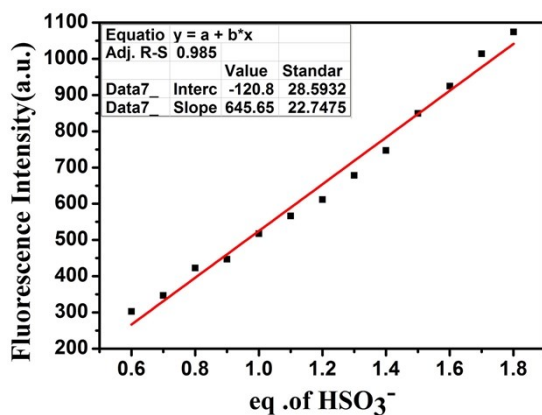


Fig. S7 The linear responses at low HSO_3^- concentrations (0.6–1.8 equiv.).

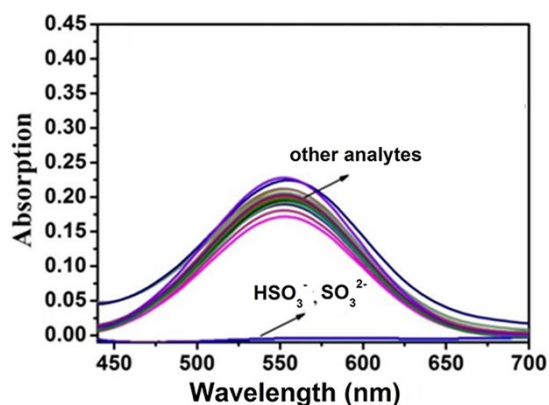


Fig. S8 UV-vis absorption changes of NPCF in the presence of different analytes (10 equiv. of Na^+ , K^+ , HS^- , Cys, Hcy, GSH, NO_3^- , CO_3^{2-} , HCO_3^- , Ac^- , SO_4^{2-} , PO_4^{3-} , F^- , Cl^- , Br^- , I^- , NO_2^- , $\bullet\text{OH}$, ONOO^- , $\bullet\text{NO}$, $\text{O}_2\bullet^-$, and H_2O_2) in HEPES buffer solution (pH = 7.4, 10 mM, containing 1 mM CTAB).

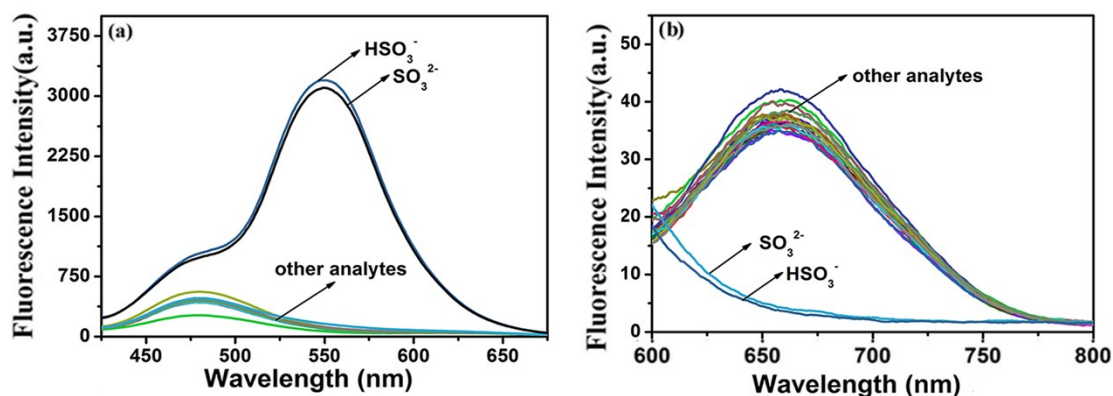


Fig. S9 Emission changes of NPCF in the presence of different analytes (10 equiv. of Na^+ , K^+ , HS^- , Cys, Hcy, GSH, NO_3^- , CO_3^{2-} , HCO_3^- , Ac^- , SO_4^{2-} , PO_4^{3-} , F^- , Cl^- , Br^- , I^- , NO_2^- , $\bullet\text{OH}$, ONOO^- , $\bullet\text{NO}$, $\text{O}_2\bullet^-$, and H_2O_2) in HEPES buffer solution (pH = 7.4, 10 mM, containing 1 mM CTAB), slits: 10/10 nm. (a) $\lambda_{\text{ex}} = 350$ nm, $\lambda_{\text{em}} = 542$ nm; (b) $\lambda_{\text{ex}} = 553$ nm, $\lambda_{\text{em}} = 653$ nm.

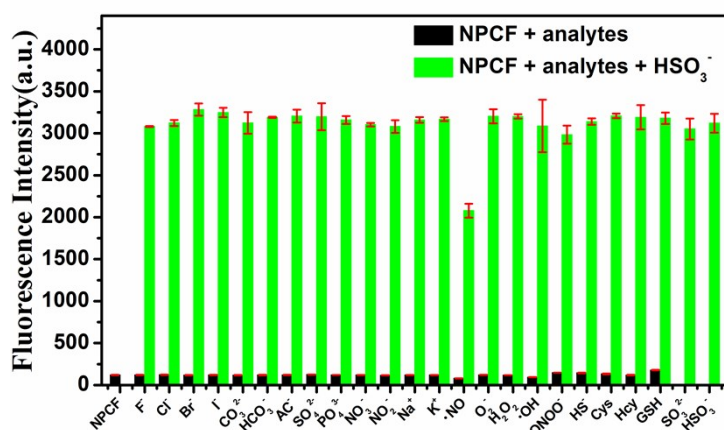


Fig. S10 Fluorescence response of NPCF (10 μM) to HSO_3^- (10 equiv.) in the presence of the different analytes. in HEPES buffer solution (pH = 7.4, 10 mM, containing 1 mM CTAB). $\lambda_{\text{ex}} = 350 \text{ nm}$, slit: 10 nm/10 nm.

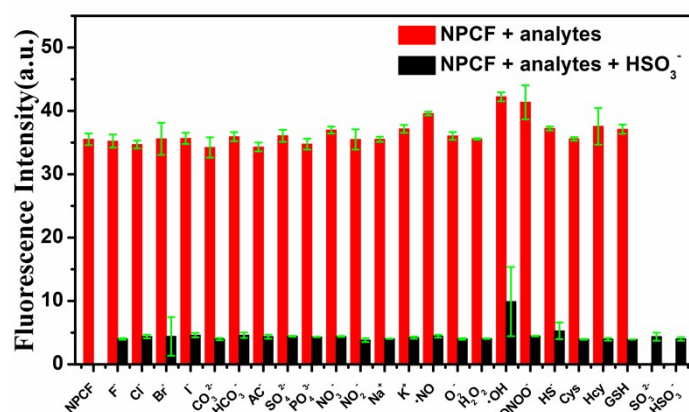


Fig. S11 Fluorescence response of NPCF (10 μM) to HSO_3^- (10 equiv.) in the presence of the different analytes in HEPES buffer solution (pH = 7.4, 10 mM, containing 1 mM CTAB). $\lambda_{\text{ex}} = 553 \text{ nm}$, slit: 10 nm/10 nm.

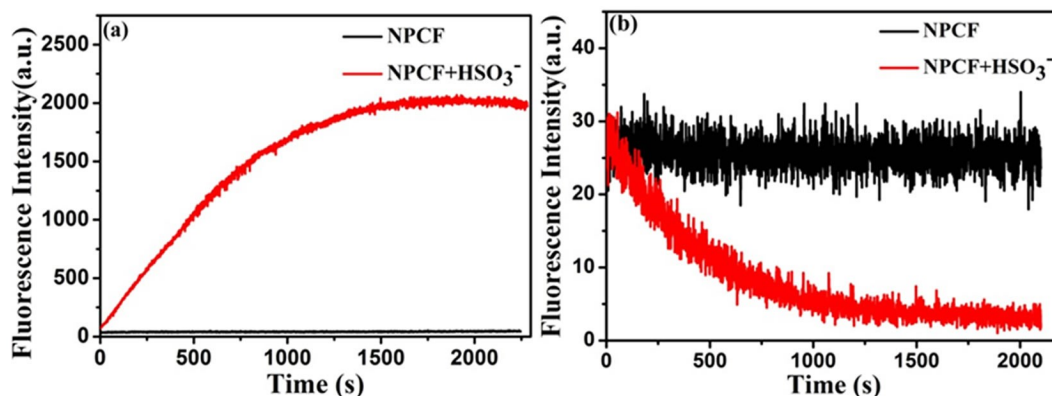


Fig. S12 Time-dependent fluorescence spectral changes of NPCF with HSO_3^- (10 equiv.) in HEPES buffer solution (pH = 7.4, 10 mM, containing 1 mM CTAB), slits: 10/10 nm. (a) $\lambda_{\text{ex}} = 350 \text{ nm}$, $\lambda_{\text{em}} = 542 \text{ nm}$. (b) $\lambda_{\text{ex}} = 553 \text{ nm}$, $\lambda_{\text{em}} = 653 \text{ nm}$.

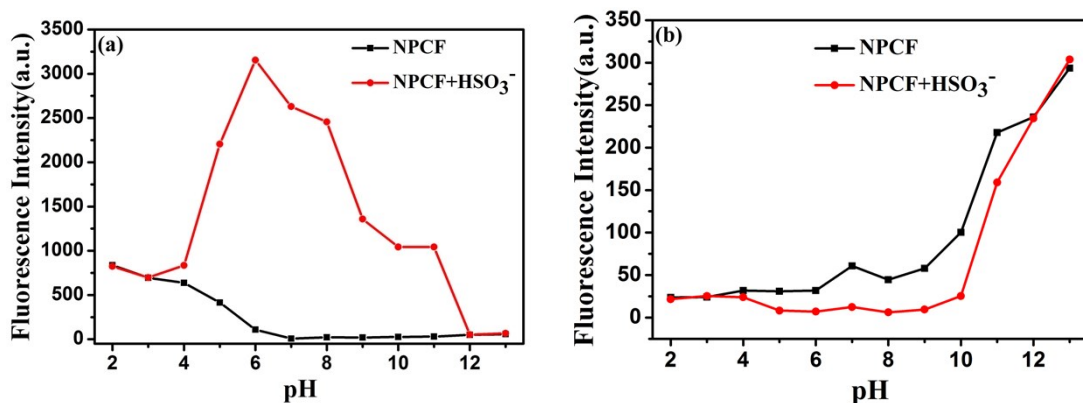


Fig. S13 The pH effect of the test solution on NPCF (10 μ M) was tested in the absence (black line) or presence (red line) of HSO₃⁻ (10 equiv.). (a) $\lambda_{ex} = 350 \text{ nm}$, $\lambda_{em} = 542 \text{ nm}$, slits: 10/10 nm. (b) $\lambda_{ex} = 553 \text{ nm}$, $\lambda_{em} = 653 \text{ nm}$, slits: 10/10 nm.

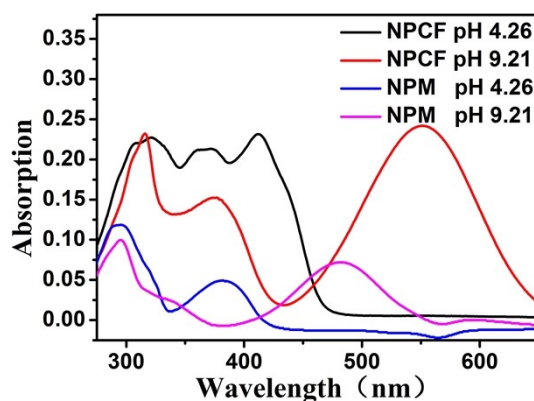


Fig. S14 UV-vis absorption spectra changes at pH 4.26 and 9.21.

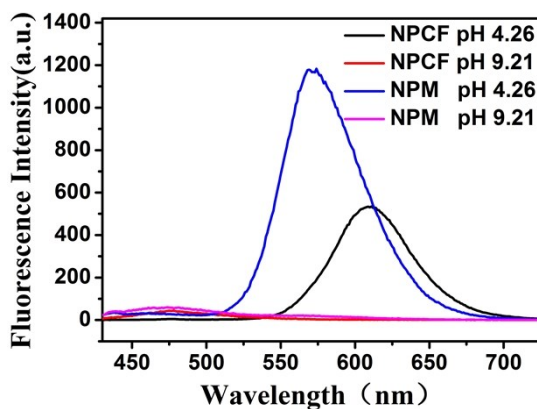


Fig. S15 Fluorescence spectra changes at pH 4.26 and 9.21. NPCF: $\lambda_{ex} = 410 \text{ nm}$, $\lambda_{em} = 610 \text{ nm}$, slits: 5/5 nm. NPM: $\lambda_{ex} = 380 \text{ nm}$, $\lambda_{em} = 573 \text{ nm}$, slits: 5/5 nm.

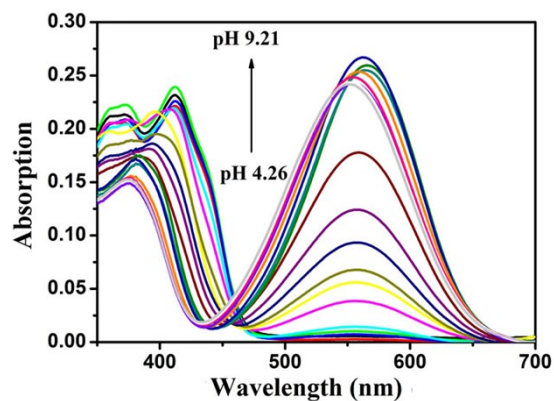


Fig. S16 Absorption spectra changes of NPCF at different pH values.

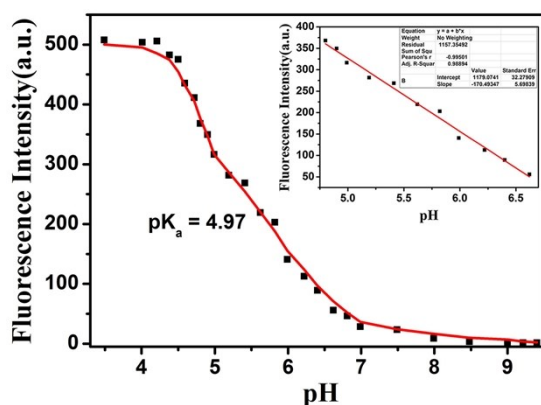


Fig. S17 The pH titration curve of NPCF plotted by fluorescence as a function of pH. Conditions: $\lambda_{\text{ex}} = 410 \text{ nm}$, slits: 5/5 nm.

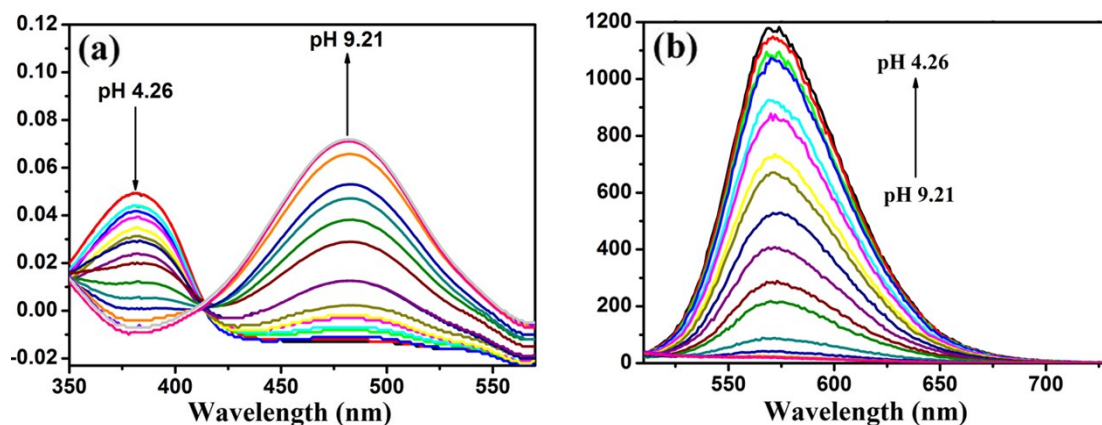


Fig. S18 (a) Absorption and (b) fluorescence spectra changes of NPM at different pH values. (b) $\lambda_{\text{ex}} = 380 \text{ nm}$, $\lambda_{\text{em}} = 573 \text{ nm}$. Slits: 5/5 nm.

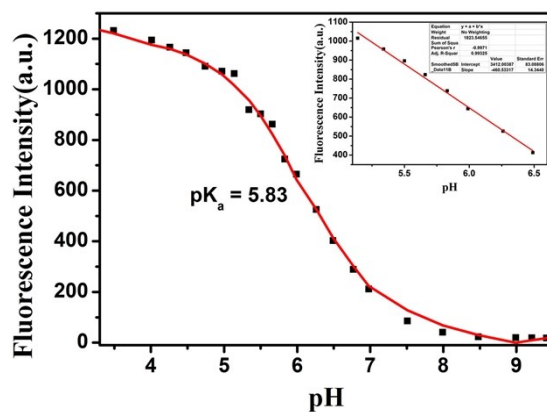


Fig. S19 The pH titration curve of NPM plotted by fluorescence as a function of pH. Conditions: $\lambda_{\text{ex}} = 380 \text{ nm}$, $\lambda_{\text{em}} = 573 \text{ nm}$, slit: 10 nm/10 nm.

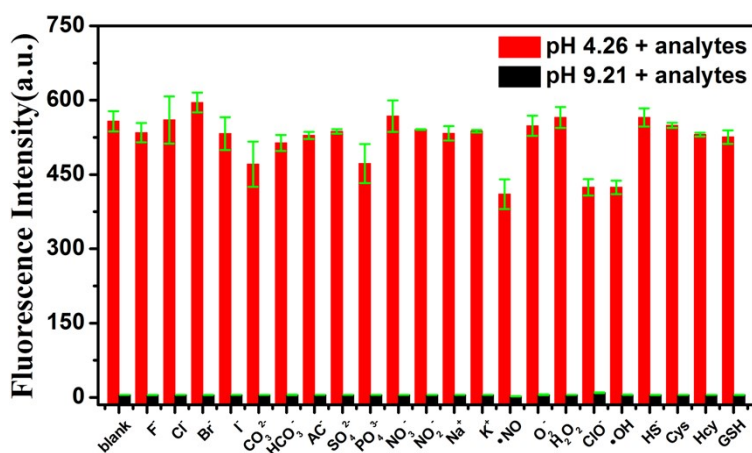


Fig. S20 The fluorescence of NPCF in pH 4.26 and 9.21 under different potential interference of interference agents. Conditions: $\lambda_{\text{ex}} = 410 \text{ nm}$, $\lambda_{\text{em}} = 610 \text{ nm}$.

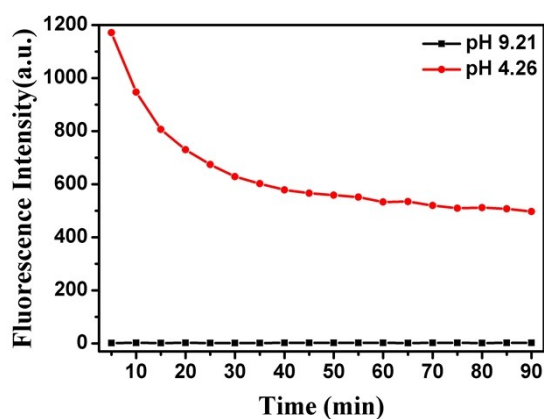


Fig. S21 The time courses of fluorescence intensity of NPCF in HEPES buffer solution (10 mM, containing 1 mM CTAB) at different pH values (4.26 and 9.21, respectively). Conditions: $\lambda_{\text{ex}} = 410 \text{ nm}$, $\lambda_{\text{em}} = 610 \text{ nm}$, slit: 5 nm/5 nm.

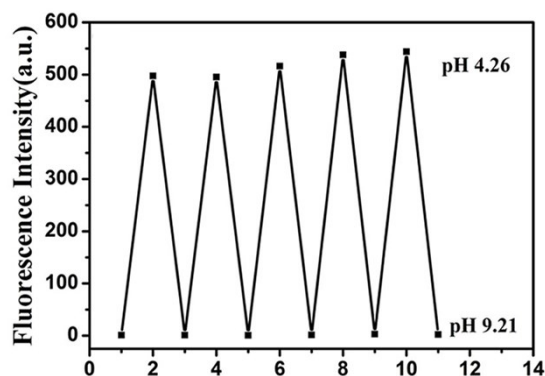


Fig. S22 Reversible fluorescence intensity ($\lambda_{em} = 610$ nm) changes of NPCF between pH = 4.26 and 9.21 in HEPES buffer solution (10 mM, containing 1 mM CTAB). Conditions: $\lambda_{ex} = 410$ nm, $\lambda_{em} = 610$ nm.

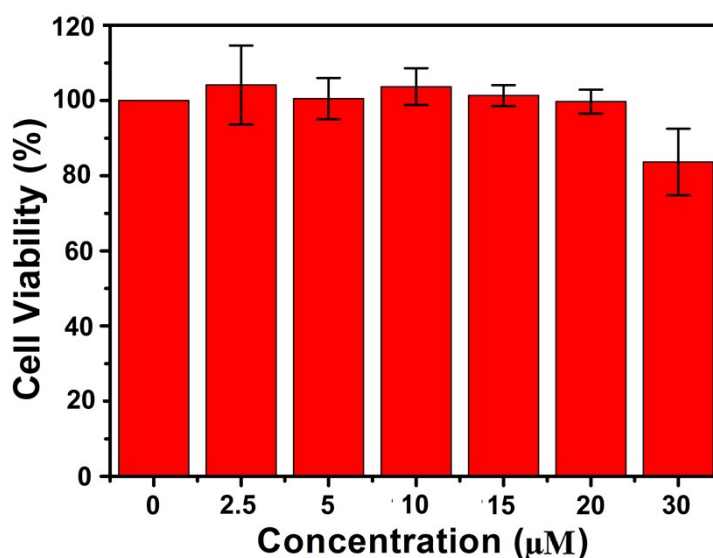


Fig. S23 Different NPCF concentrations (0, 2.5 μ M, 5 μ M, 10 μ M, 15 μ M, 20 μ M and 30 μ M) were tested in Hela cells for toxicity.

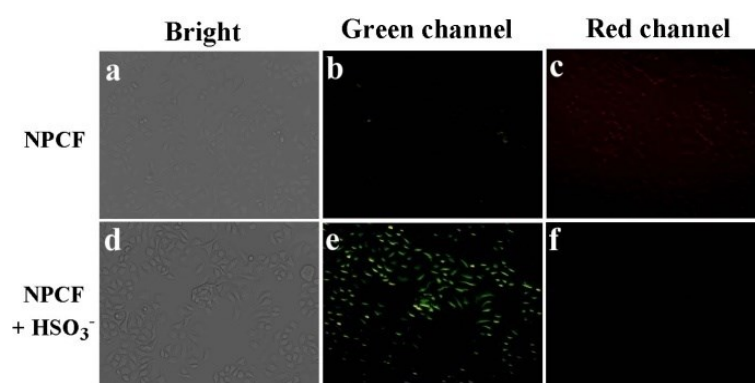


Fig. S24 Fluorescence images of MCF-7 cells. (a, b and c) cells were incubated with NPCF (10 μ M) for 0.5 h; (d, e and f) images of cells after treatment with probe NPCF (10 μ M) for 0.5 h and then treatment of the cells with 100 μ M of HSO₃⁻ for 1

h. (a and d) Bright field images; (b and e) green emission of NPCF; (c and f) red emission of NPCF.

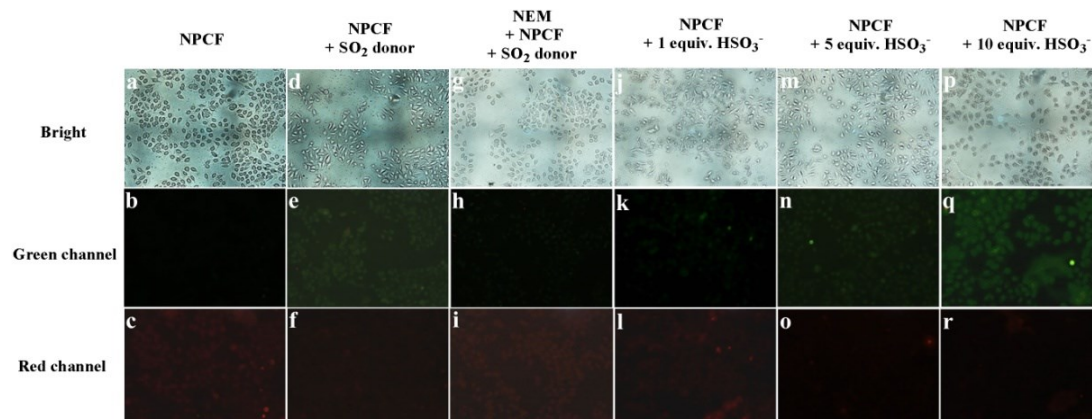


Fig. S25 Fluorescence images of MCF-7 cells. The cells were incubated with NPCF (10 μM) for 0.5 h (a, b, and c) and 100 μM of SO_2 donor for 1 h (d, e and f). The cells were treated with 1 mM of NEM for 0.5 h, incubated with NPCF (10 μM) for 0.5 h, and then treated with 100 μM of SO_2 donor for 1 h (g, h and i). MCF-7 cells were incubated with NPCF (10 μM) for 0.5 h and treated with several concentrations of HSO_3^- for 1 h (j–r).

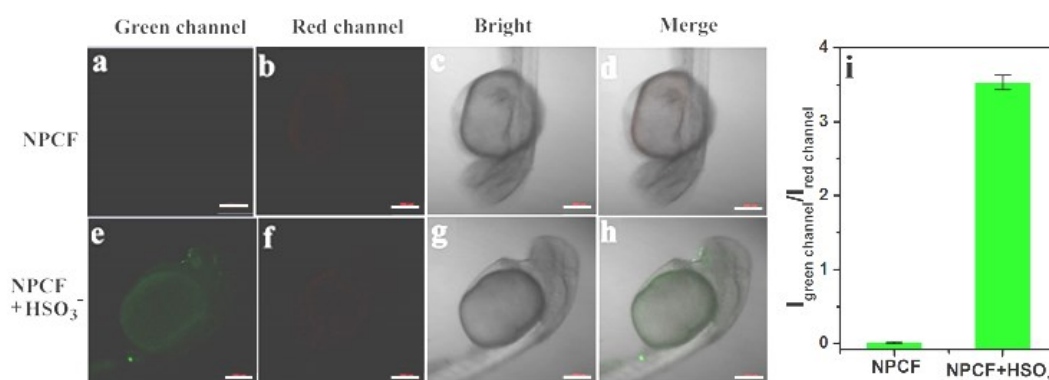


Fig.S26 Confocal fluorescence images of zebrafish using a 10 \times objective. (a–d) NPCF (10 μM) and zebrafish were incubated for 0.5 h. (e–h) NPCF (10 μM) and zebrafish were incubated for 0.5 h, and then treated with HSO_3^- (100 μM) for 1 h. (i) Relative pixel intensity of $I_{\text{green channel}}/I_{\text{red channel}}$ for detecting HSO_3^- . (a and e) $\lambda_{\text{ex}} = 405$ nm, $\lambda_{\text{em}} = 520$ nm–560 nm; (b and f) $\lambda_{\text{ex}} = 552$ nm, $\lambda_{\text{em}} = 630$ –670 nm. Scale bar is 200 μm .

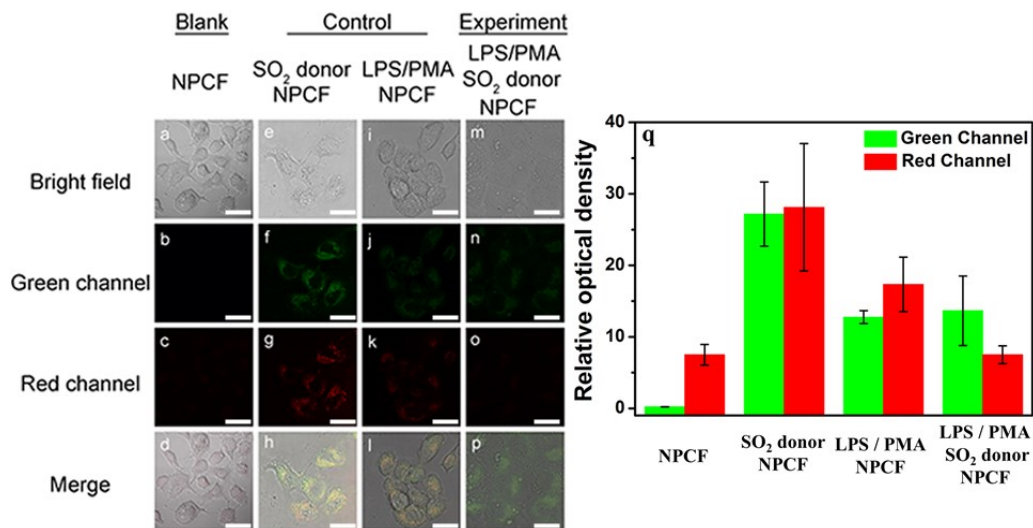


Fig. S27 (a–d) EC1 cells were incubated with NPCF (10 μ M) for 0.5 h. (e–h) EC1 cells were incubated with SO₂ donor (100 μ M) for 1 h, and then incubated with NPCF (10 μ M) for 0.5 h. (i–l) EC1 cells were incubated with LPS (10 mg/L) for 12 h and PMA (1 μ g/mL) for 1 h, and then incubated with NPCF (10 μ M) for 0.5 h. (m–p) EC1 cells were incubated with LPS (10 mg/L) for 12 h and PMA (1 μ g/mL) for 1 h, followed by adding SO₂ donor (100 μ M) for 1 h, and finally incubated with NPCF (10 μ M) for 0.5 h. (q) Relative pixel intensity of green channel (b, f, j and n, λ_{ex} = 405 nm, λ_{em} = 520 nm–560 nm) and red channel (c, g, k and o, λ_{ex} = 552 nm, λ_{em} = 630–670 nm). Scale bar is 25 μ m.

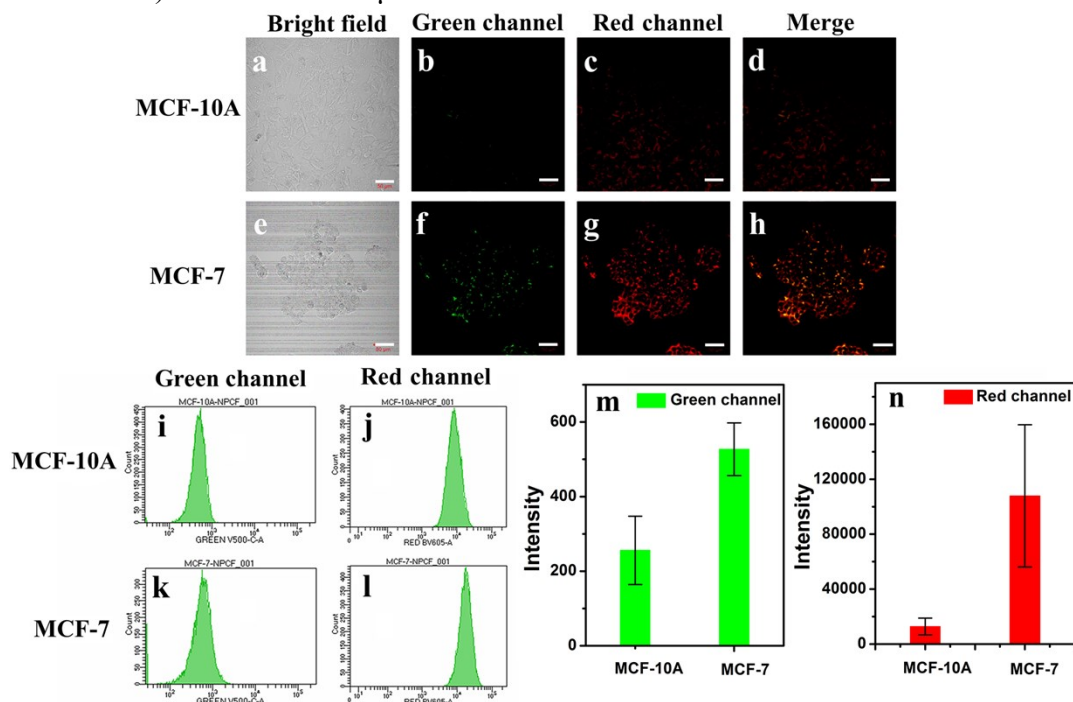


Fig. S28 Confocal fluorescence images of cancer cells vs normal cells. NPCF were incubated with MCF-10A cells (a–d) and MCF-7 cells (e–h) for 0.5 h, respectively. Scale bar is 25 μ m. (i–l) Flow cytometry analysis of (a–h). (m) The mean intensity of green channel (i and k, λ_{ex} = 405 nm, λ_{em} = 520 nm–560 nm) and (n) red channel (j and l, λ_{ex} = 552 nm, λ_{em} = 630–670 nm) on the flow cytometry analysis.

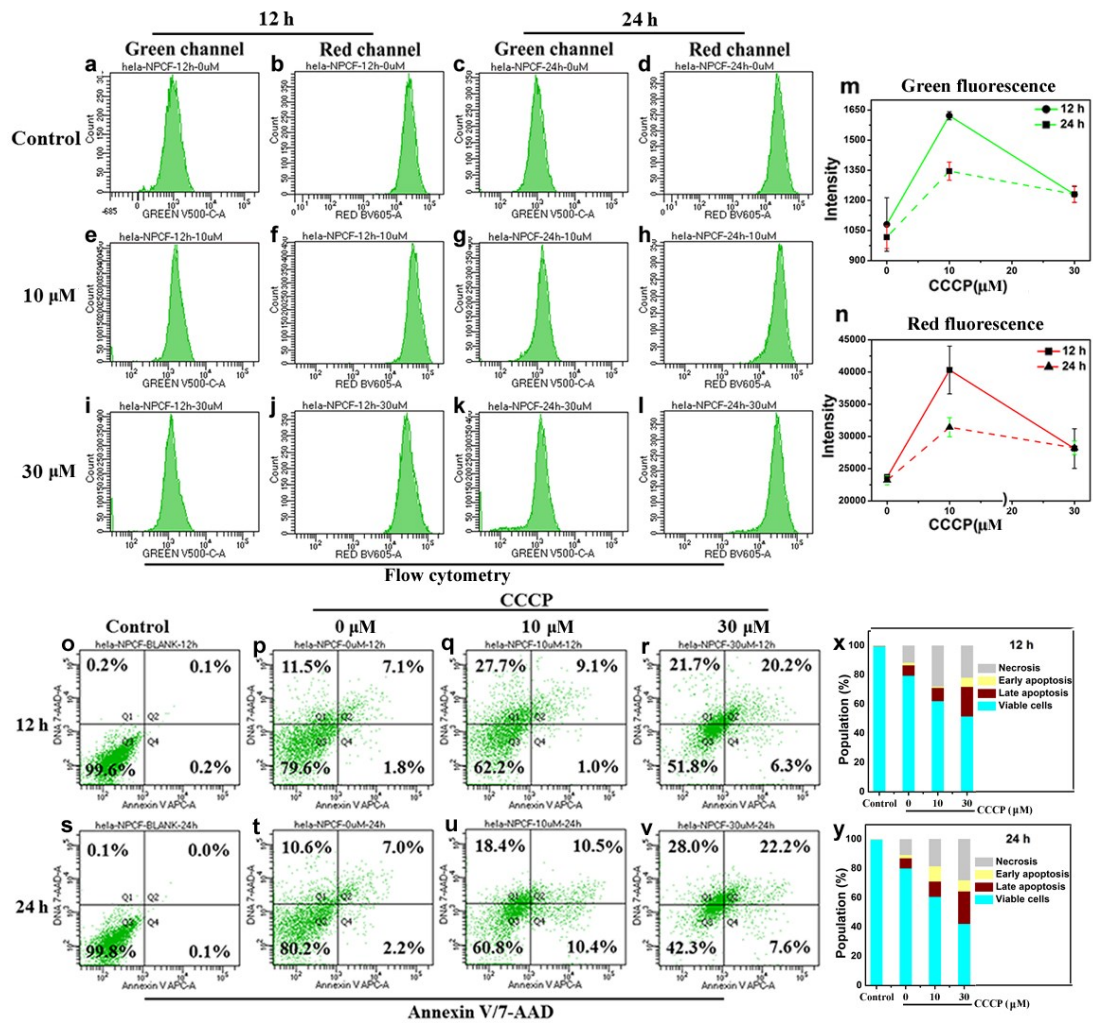


Fig.S29 Experiments of SO₂ and pH changes in CCCP-induced apoptosis. Flow cytometry analysis of (a–n), different concentrations of CCCP (a–d, 0 μM; e–h, 10 μM; i–l, 30 μM) were co-incubated with the cells for 12h (a, b, e, f, i and j) or 24 h (c, d, g, h, k and l), respectively, followed by separately adding NPCF (10 μM) and incubating for 0.5 h, and then analyzed by flow cytometry. (m and n) The green channel (a, e, i, c, g and k, λ_{ex} = 405 nm, λ_{em} = 520 nm–560 nm) and red channel (b, f, j, d, h and l, λ_{ex} = 552 nm, λ_{em} = 630–670 nm). (o–v) Annexin V/7-AAD analysis of apoptosis of CCCP at different concentrations (p and t, 0 μM; q and u, 10 μM; r and v, 30 μM) and different culture time (o–r, 12 h; s–v, 24 h). (x–y) The population of necrosis (Q1), early apoptosis (Q4), late apoptosis (Q2), and viable cells (Q3) for 12h (x) or 24h (y) in the Annexin V/7-AAD analysis of apoptosis (o–v).

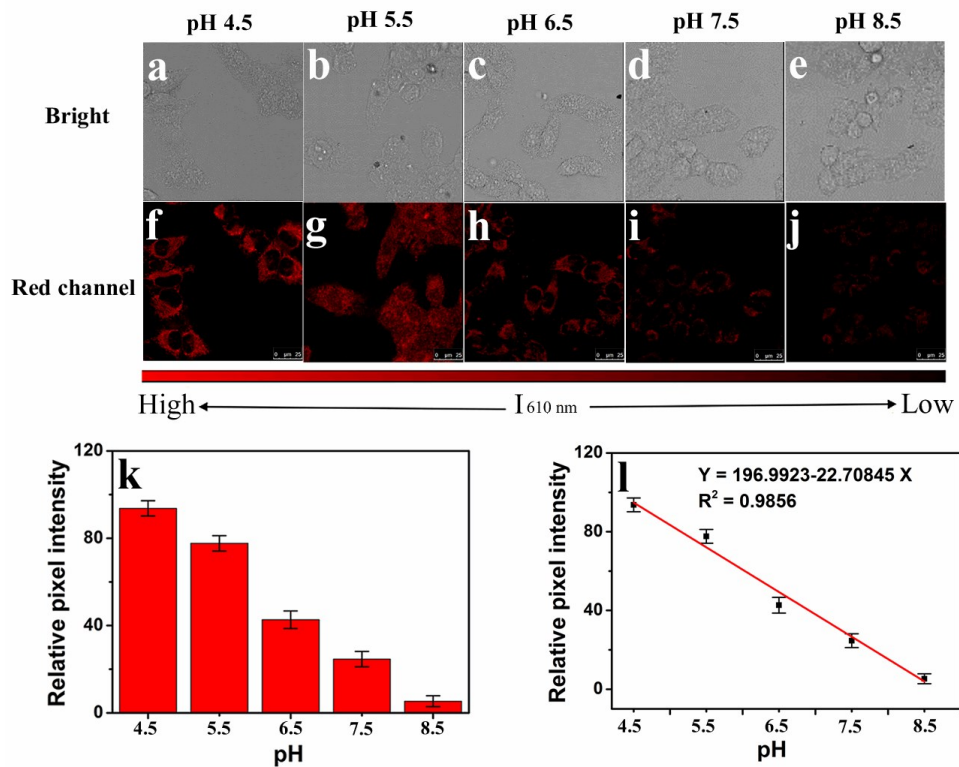


Fig.S30 (a–j) Confocal fluorescence images of HeLa cells and NPCF (10 μM) were treated with different pH PBS buffers (pH 4.5, 5.5, 6.5, 7.5 and 8.5) for 0.5 h, respectively. (k) Relative pixel intensity of red channel ($\lambda_{ex} = 552$ nm, $\lambda_{em} = 630$ – 670 nm) in different pH PBS buffers. (l) The linear responses in different pH PBS buffers. Scale bar is 25 μm